UNIVERSITÀ DEGLI STUDI DI PADOVA

DIPARTIMENTO DI BIOLOGIA

Corso di Laurea magistrale in Molecular Biology

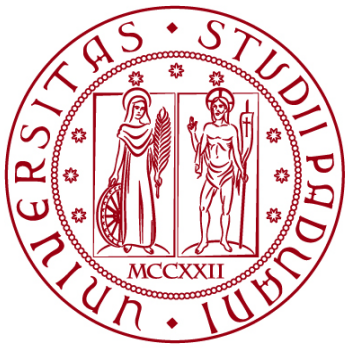

TESI DI LAUREA

Mitophagy and release of mitochondria derived vesicles in cellular models of inducible unfolded protein accumulation in mitochondrial matrix and intermembrane space.

Relatore: Prof. Luca Scorrano
DIPARTIMENTO DI BIOLOGIA

Laureanda:Delaram Nejadfard

ANNO ACCADEMICO 2022/2023

Content;

Table of Figures

Abbreviations

AA	Antimycin A
ATFS-1	Activating Transcription Factor associated with Stress-1
ADP	Adenosine diphosphate
ATP	Adenosine triphosphate
ANOVA	Analysis of Variance
BCL2	B-cell lymphoma 2
BNIP3	BCL2 interacting protein 3
BSA	Bovine serum albumin
CCCP	Carbonyl cyanide m-chlorophenyl hydrazine
CRISPR–Cas9	Clustered Regularly Interspaced Short Palindromic Repeats-CRISPR-associated protein 9
CJ	Cristae junctions
CMV	Cytomegalovirus
DMEM	Dulbecco's Modified Eagle Serum
DNA	Deoxyribonucleic Acid
Drp1	Dynamin-related protein
EGFP	Enhanced green fluorescent protein
ER	Endoplasmic reticulum
ETC	Electron transport chain
EV	Empty vector
FAD	Flavin Adenine Dinucleotide
FAST	Fluorescence-Activating and absorption-Shifting Tag
FBS	Fetal Bovine Serum
Fis1	Mitochondrial fission 1 protein
FUN14	Formation of Organellar Networks 14
FUNDC1	FUN14 domain-containing 1
GFP	Green Fluorescent protein
GTP	Guanosine Triphosphate
HBSS	Hank's Balanced Salt Solution
HEPES	4-(2-Hydroxyethyl)piperazine-1-ethanesulfonic acid

HSD	Honestly Significant Difference
IMM	Inner mitochondrial membrane
IMS	Intermembrane Space
ISR	Integrated Stress Response
MCU	Mitochondrial Calcium Uniporter
MDVs	Mitochondrial-derived vesicles
MEF	Mouse Embryonic Fibroblast
MFF	Mitochondrial fission factor
Mfn1	Mitofusin 1
Mfn2	Mitofusin 2
MID49/51	Mitochondrial Dynamics Protein of 49 kDa/51 kDa
mPTP	Mitochondrial permeability transition pore
mtDNA	Mitochondrial DNA
NA	Numerical aperture
NADH	Nicotinamide Adenine Dinucleotide (NAD) + Hydrogen (H)
OMM	Outer mitochondrial membrane
OPA1	Optic Atrophy 1
OPTN	Optineurin
OXPHOS	Oxidative phosphorylation
PARL	Presenilin-associated rhomboid-like protein
PBS	Phosphate-buffered saline
PCR	Polymerase Chain Reaction
PD	Parkinson's disease
PDH	Pyruvate dehydrogenase
PFA	Paraformaldehyde
PHEM	PIPES-HEPES-EGTA-Magnesium chloride
PINK1	Phosphatase and tensin homolog-induced putative kinase 1
Rho7	Rhomboid-7
RING	Really interesting new gene
ROI	Region of Interest
TCA	Tricarboxylic Acid
TF	The Twinkle Factory

TIM	Translocase of the inner membrane
TOM	Translocase of the outer membrane
ΔΨm	Mitochondrial membrane potential

Abstract

Accumulation of mitochondrial unfolded protein is a pathological threat insufficiently mentioned about the pathophysiological contribution and intrinsic counter mechanisms. This accumulation leads to mitochondrial dysfunction and cellular stress. Hence, in response to this stress, mitochondrial selective autophagy known as mitophagy is potentially induced as a protective mechanism to eliminate the damaged mitochondria and aggregates unfolded protein (1). As another quality control machinery of mitochondria, mitochondria-derived vesicles (MDVs) can also be released from the damaged mitochondria. MDVs are small vesicles derived from the mitochondrial membrane that contain various cargo molecules. (2)

During this thesis the mitochondrial unfolded protein model was generated by targeting luciferase mutant, which has been shown as unfolded proteins, into mitochondria. Moreover, Immunofluorescence techniques were used during this project in order to visualize and differentiate MDVs. Also, in order to track the mitophagy, we have generated an optimized system utilizing a different mitophagy sensor.

Our results demonstrated well-defined MDVS including PDH-positive MDVs and TOM20-Positive MDVs. We have also proved that the enhanced system provides a valuable alternative mitophagy sensor in which mitochondria-targeting EGFP conjugated mTagBFP2 can be used instead of mCherry and in order to take advantage of the blue color instead of red.

Introduction

Mitochondria

Structure of mitochondria

Mitochondria, double-membrane-bound organelles, are primarily involved in energy conversion through oxidative phosphorylation (OXPHOS). Mitochondria re consisted of an outer membrane (OMM), an inner membrane (IMM), and the space lying between OMM and IMM or inside of IMM, called as intermembrane space and matrix, respectively (Figure 1). The two membranes have distinct structures and functions. The IMM forms cristae structures and serves as the site for oxidative phosphorylation, housing the electron transport chain and various channels, such as the mitochondrial Ca^{2+} uniporter and the inner membrane anion channel (3). On the other hand, the OMM contains fewer proteins encoded by the nucleus, including pore-forming proteins, enzymes, and proteins involved in fission and fusion processes (4). Unlike the IMM, the OMM is porous, resulting in the absence of a membrane potential.

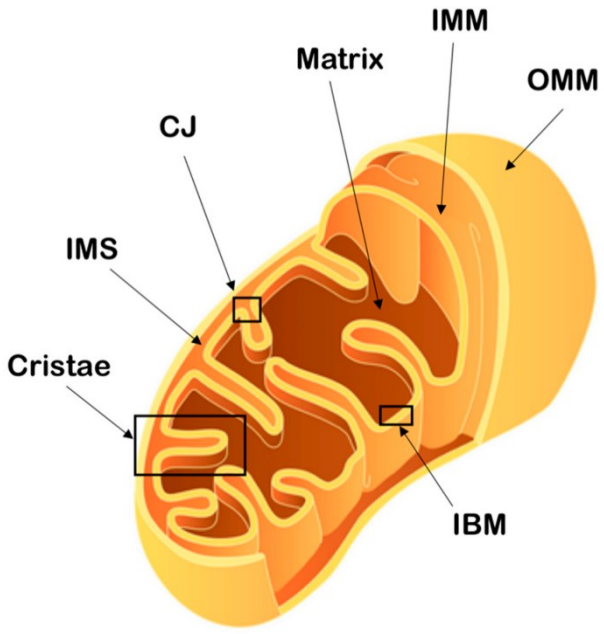

Figure 1; Schematic representation of mitochondrial architecture. The outer mitochondrial membrane (OMM), inner mitochondrial membrane (IMM), inner boundary membrane (IBM), cristae junctions (CJ), intermembrane space (IMS), cristae and mitochondrial matrix are indicated. Figure obtained from reference (5).

The matrix of mitochondria maintains a higher pH than neutral (around 7.8), which is reflected the electrochemical gradient formed by oxidative phosphorylation. Mitochondrial matrix is also the region housing mitochondrial DNA (mtDNA) and facilitating mtDNA replication and transcription. The intermembrane space, approximately 20 nm wide, allows small molecules and ions to be entry by free diffusion. Other mitochondrial IMS proteins was transported by the translocase of the outer membrane (TOM20) complex. Theres refilled by proteins regulating mitochondrial respirations, metabolic functions, and apoptosis initiation in IMS (4).

Functions of mitochondria

Mitochondria are responsible for generating adenosine triphosphate (ATP) through the process of oxidative phosphorylation (OXPHOS) at the IMM. This ATP production is depending on the electrochemical gradient across the IMM. This gradient is generated by the transfer of electrons through respiratory complexes integrated in the IMM and the movement of protons from matrix to IMS. The passive movement of protons generate electrochemical gradient and used by ATP synthase that enzyme enables the conversion of adenosine diphosphate (ADP) into ATP.

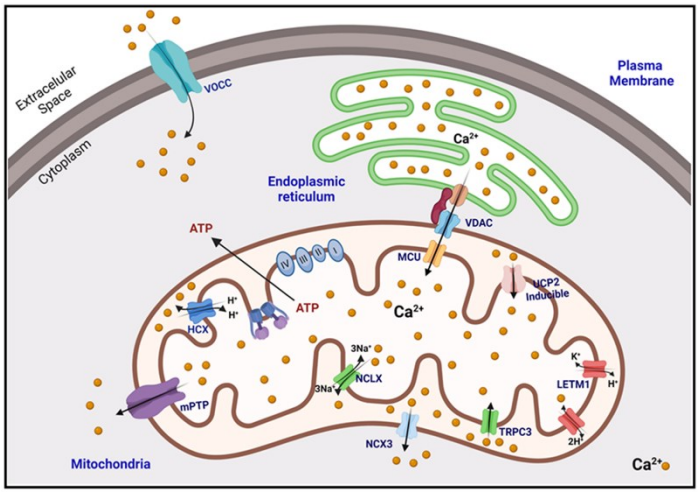

Figure 2; The fundamental concept of calcium transport within cells follows a structured model. Firmly rooted within the outer mitochondrial membrane (OMM), one encounters the voltage-dependent transports (VDACs). Their primary role involves the uptake of calcium ions from the cytosol and their relocation to the intermembrane space (IMS). Nevertheless, it is noteworthy that these transports sometimes act to exclude calcium ions. Another set of participants in this intricate process includes the NCX3 transporter and the mitochondrial permeability transition pore (mPTP), which can also mediate calcium exclusion. On a parallel note, residing within the inner mitochondrial membrane (IMM), an array of transporters undertakes the task of steering calcium ions towards the matrix. Among these transporters, a key player is the mitochondrial Ca2+ uniporter complex (MCU). This complex represents a universally present uniporter mechanism, allowing for the regulated passage of calcium ions into the matrix. Figure obtained from reference (7).

Mitochondria import Ca^{2+} into the mitochondrial matrix from the endoplasmic reticulum using a mitochondrial calcium uniporter (6). The ability to buffer calcium is crucial for processes including neurotransmitter release, neuron generation, plasticity, muscle contraction, and Ca^{2+} signaling. Elevated Ca^{2+} concentrations in the matrix, resulting from these processes, positively influence ATP generation by up-regulating oxidative phosphorylation to meet the energy demands of these calcium-dependent activities. However, once the Ca^{2+} import was over the capacity of mitochondria, Ca^{2+} overload triggers apoptosis, a programmed cell death process. During apoptosis, cytotoxic proteins, including cytochrome c, are released from the IMS of mitochondria into the cytosol. This release initiates caspase activation, leading to cell death (7).

Glycolysis and Krebs Cycle

Glycolysis is the first step in cellular respiration, the process by which cells generate energy from glucose. It occurs in the cytoplasm of the cell and doesn't require oxygen. Through glycolysis processes, glucose is sequentially converted and finally resulted in the generation of pyruvate together with the generation of 2 ATP and 2 NADH.

The Krebs cycle, also known as the citric acid cycle or tricarboxylic acid cycle (TCA cycle), is a crucial metabolic pathway that takes place within the mitochondria matrix. The metabolic cycle begins from pyruvate transported from the cytoplasm into the mitochondrial matrix. Inside the matrix, pyruvate undergoes a series of reactions that contribute to produce metabolites, such as NADH, FADH2 utilized for electron transport chains (8).

NADH and FADH2, formed during different stages of the cycle, carry high-energy electrons to the electron transport chain (ETC) embedded in the inner mitochondrial

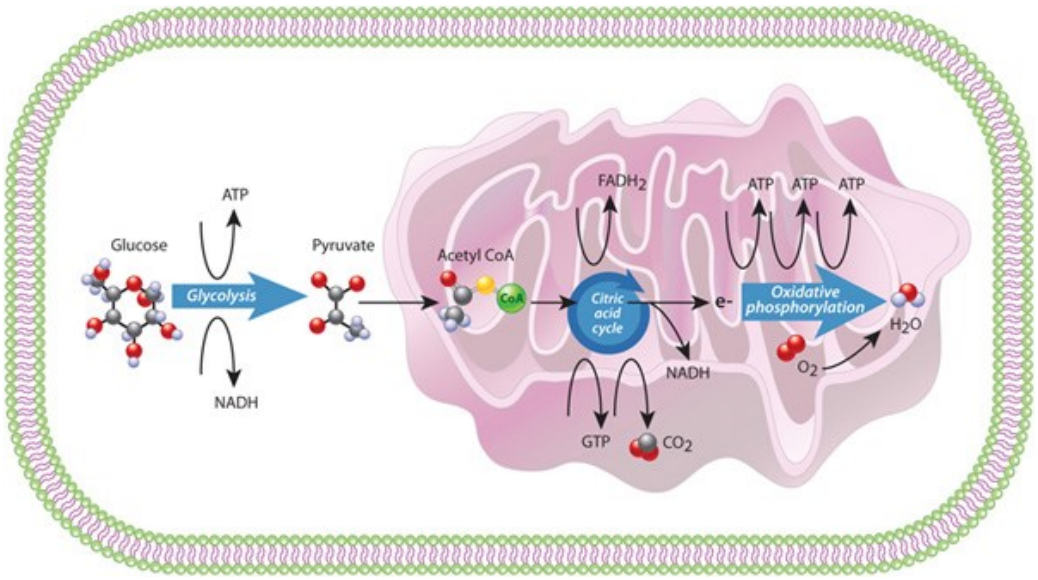

Figure 3; Metabolism in a eukaryotic cell: Glycolysis, the citric acid cycle, and oxidative phosphorylation

Glycolysis takes place in the cytoplasm. Within the mitochondrion, the citric acid cycle occurs in the mitochondrial matrix, and oxidative metabolism occurs at the internal folded mitochondrial membranes (cristae). Figure obtained from reference (8).

membrane. This is a crucial step for oxidative phosphorylation, where the bulk of ATP is generated. The cycle ends when the oxaloacetate used at the beginning is regenerated, allowing the cycle to continue as long as there are available substrates (8).

Oxidative Phosphorylation

Oxidative phosphorylation takes place within the mitochondrial matrix and is the predominant process for providing the most part of cellular ATP. This process requires oxygen and involves a series of ETC reactions coupled with the synthesis of ATP. During the series of ETC reaction through mitochondrial respiratory chains, protons H^+ is actively pumped across the IMM from the matrix to the IMS, generating a proton gradient. The protons gradient allows and drives the rotation of ATP synthase complex with couples to ADP conversion into ATP. (5)

Mitochondrial Quality Control Processes

Mitochondria form extensive interconnected networks within cells and owing to their susceptibility to oxidative damage, necessitate quality control mechanisms to

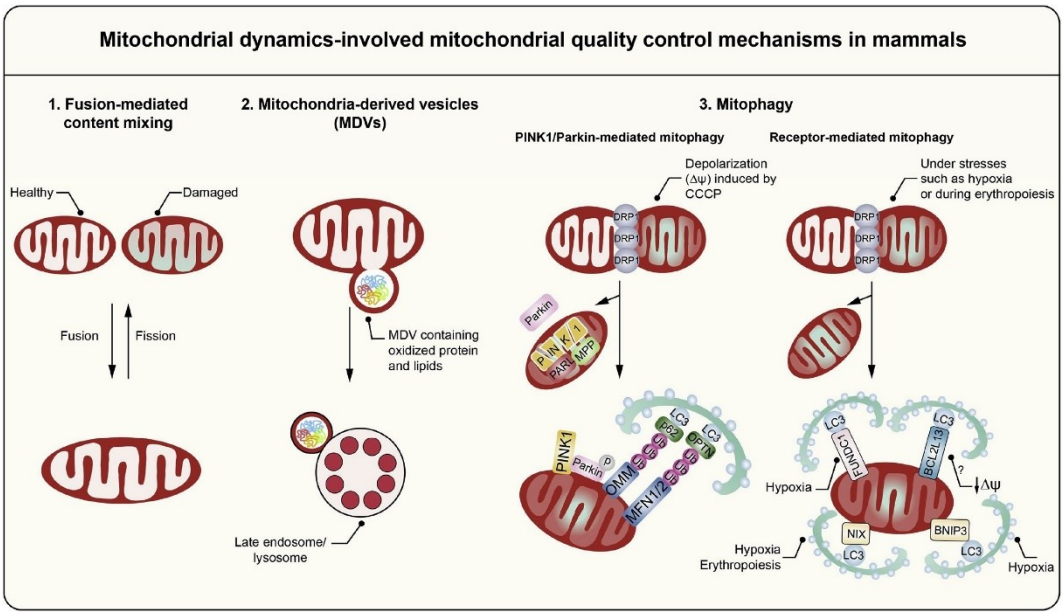

Figure 4; Mitochondrial quality control mechanisms involving mitochondrial dynamics. Mitochondria harbor a network of surveillance mechanisms encompassing 1. fusion-mediated function complementation, 2. mitochondria-derived vesicles, and 3. mitophagy processes to protect mitochondrial homeostasis from increasing degrees of damage. Specifically, fusion-mediated functional complementation and mitochondria-derived vesicles constitute the first line of defense against mild mitochondrial impairment. Figure obtained from reference (9).

ensure efficient functioning. Severe mitochondrial damage leads to apoptosis, however, to counteract this, various repair and damage control mechanisms were operated within mitochondria, which will be explored below.

Fission and Fusion

Mitochondria are highly dynamic organelles, continually undergoing two opposing processes known as fission and fusion (Figure 5). These processes allow the movement of mitochondrial contents between mitochondria, ensuring a homogenous population.

During fusion, the outer mitochondrial membrane (OMM) and inner mitochondrial membrane (IMM) between two mitochondria was connected simultaneously, promoting the mixing of contexts in the IMS and mitochondrial matrix. Mitochondrial proteins OPA1, Mfn1, and Mfn2 are essential mediators of this

process. Mfn1 and Mfn2 are transmembrane GTPases embedded in the OMM, facilitating outer membrane fusion, while OPA1, a dynamin-related GTPase embedded in the IMM, mediates inner membrane fusion. Notably, mutations in OPA1 and Mfn2 have been associated with specific diseases (10), suggesting that mitochondrial fusion process contribute the health of cells beyond mitochondria per se and counteract pathological processes in diseases.

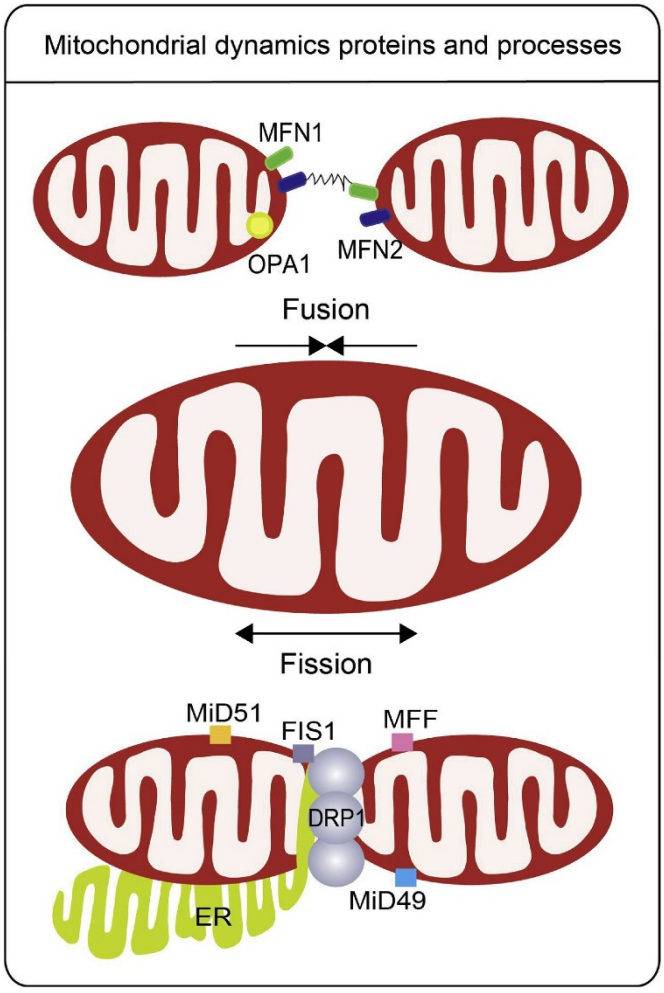

Figure 5; Mitochondrial fusion joins two mitochondria together, while fission separates one into two. Fusion is coordinated on the OMM by the mitofusins (MFN1 and MFN2), and on the IMM by optic atrophy 1 (OPA1). Fission begins when the endoplasmic reticulum (ER) is recruited to the constriction site, marked by mtDNA. Next, multiple OMM-bound proteins (FIS1, MFF, MID49 and MID51) recruit DRP1 to the surface of the mitochondria, aiding in ER-mediated constriction. Figure obtained from reference (9).

Studies using mouse embryonic fibroblasts (MEFs) with null alleles of mitofusins have shown that outer and inner mitochondrial membrane fusion is disappeared in these cells, however, OPA1-null MEFs still exhibit outer mitochondrial membrane fusion(12), although inner membrane fusion fail to operate (11;12). Mitofusin 1 mediates oligomerization, and GTP hydrolysis is believed to facilitate conformational changes that enable membrane fusion (11; 13). On the other hand, fission is the process by which daughter mitochondria are generated through the division of one mitochondrion. Mitochondrial fission is a dynamic process that is required to maintain mitochondrial quality and cellular health through a variety of mechanisms. First, it allows the removal of damaged parts in the mitochondria. When specific mitochondrial components are damaged due to oxidative stress, protein misfolding, or other insults, fission helps to clear

and eventually dispose of these non-functional sites thus preventing their deleterious effects on overall organelle well-being. Secondly, fission contributes to the separation of healthy and damaged mitochondria. By forming specific compartments, functional mitochondria can efficiently meet the energy needs of the cell, while repairing damaged counterparts for degradation(14). Finally, fission plays an important role in targeted mitophagy on, in the process of selective destruction. Small mitochondria generated by fission are easily recognized and engulfed by autophagosomes, thus facilitating their specific removal by lysosomal degradation. This fission process is conducted by dynamin-related protein (Drp1) in the cytosol, along with mitochondrial Drp1 adaptor proteins MID49, MID51, Fis1 and MFF (14). Drp1 is recruited to mitochondria by these Drp1 adaptors for initiate mitochondrial constriction, leading to division of mitochondrion (15). MFF, separate from Fis1, is a well-established Drp1 receptor that mediates Drp1 recruitment to mitochondria (15).

Mitochondrial-derived Vesicles

Resent research has demonstrated that defective components in mitochondria can be directly eliminated by being transported to the lysosome via mitochondrial-derived vesicles (MDVs) (16).

These vesicles MDVs form by budding from mitochondrial tubules and selectively sequester mitochondrial cargos under normal conditions, serving as a quality control mechanism. Therefore, MDVs have many varieties of types and cargos. Among these MDVs types, the two types of MDVs, mitochondrial outer membrane protein TOM20 positive and mitochondrial matrix protein pyruvate dehydrogenase (PHD) negative MDVs (TOM20+ MDVs) and TOM20 negative but PDH positive

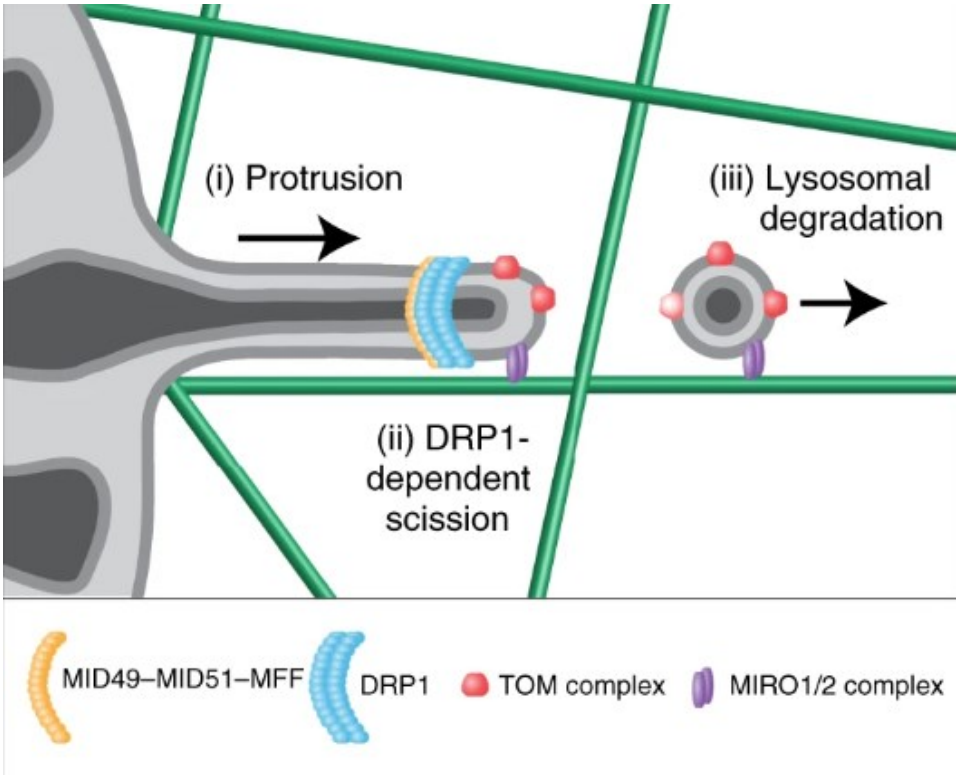

Figure 6; Model of GTPase-driven biogenesis of MDVs. (i) MDV formation is initiated by MIRO1/2 complex-dependent microtubule-mediated pulling of thin membrane protrusions. (ii) DRP1 is recruited by the redundant DRP1 receptors MID49, MID51 and MFF, and assembles into small foci close to the tip. (iii) MDV formation is completed by DRP1-mediated scission. Unprocessed blots and numerical source data, including exact P values and test statistics, are provided. Figure obtained from reference (17).

MDVs (PDH+ MDVs) are well-found and well-known general MDVs, although functional distinction among each MDVs remain poorly unknown. At least, MDVs formation is particularly upregulated in the presence of oxidative stress, allowing the organelle to remain intact while eliminating oxidized mitochondrial proteins.

This pathway is a selective process in mitochondrial quality control (QC) and is situated in the milder stress positioned between mitochondrial proteases and mitophagy. The molecular events that drive MDV formation include MIRO1/2-dependent microtubule-mediated pulling of thin membrane protrusions, recruitment of DRP1 by redundant DRP1 receptors, and DRP1-mediated scission. The MDVs are then transported to their target destinations, such as the endolysosomal pathway. Previously, the CRISPR–Cas9 technology was used to reveal that knockout of DRP1 or the combined loss of its receptors results in a total ablation of MDV formation(17). Additionally, phosphatidic acid is crucial for the regulation of DRP1 recruitment, assembly and activity of Drp1 (18), and biogenesis of TOM+ MDVs, and the ratio of phosphatidic acid and cardiolipin in TOM+ MDVs is highly distinct from the outer mitochondrial membrane (OMM) (17).

Reciprocal interactions with other organelles modulate mitochondrial division in a complex interplay (19, 20). In contrast to the binary mid-zone or peripheral mitochondrial fission process, TOM+ MDVs do not contain mtDNA and only carry a subset of mitochondrial proteins (17).

Although PARKIN, a well-defined protein as key regulator for conducting mitochondrial targeting autophagy, does not regulate the steady-state MDV pathway, previous work has documented roles for PARKIN as positive regulators of a subset of oxidative stress-induced MDVs (21) and negative regulators of inflammation-induced MDVs (22). Additional QC mechanisms report the selective remodeling of the mitochondrial proteome, with characteristics reminiscent of MDVs the DRP1- and PARKIN-dependent removal of toxic protein aggregates in yeast and mammals (23).

Mitophagy and The Mechanism of Mitophagy

When mitochondria experience severe damage beyond the repair capabilities of a subset of mitochondrial proteins, a process called mitophagy comes into play to eliminate the entire damaged organelle by using autophagy process. Mitophagy is a critical mechanism that ensures the optimal production of cellular energy by selectively degrading dysfunctional mitochondria, thereby preventing the toxic accumulation of damaged components. In the upcoming section, we will delve into

the intricacies of this essential process and explore how cells maintain their mitochondrial health through mitophagy.

PINK1 and Parkin dependent mitophagy

The PTEN-induced kinase 1 (PINK1) is a responsible gene showing casual mutations in autosomal recessive early-onset Parkinson's disease, and more than 50 mutation sites have been identified in the kinase and carboxyl-terminal regulatory domains (some of these sites are depicted in Figure 8).

PINK1 is initially synthesized in the cytosol and subsequently imported into the mitochondria through the TOM complex, facilitated by a mitochondrial targeting sequence at its N-terminus. Despite being ubiquitously expressed, PINK1 is maintained at low levels under normal physiological conditions due to degradation processes. The Rhomboid-7/Presenilin-associated rhomboid-like protein (Rho7/PARL) processing in the cytosol and degradation by the protease Lon in the mitochondrial matrix help regulate PINK1 levels (24), PINK1 under basal levels is expressed at very low levels and also can be found in cytosol and endoplasmic reticulum (25).

Parkin

Parkin is classified as a cytosolic E3 ubiquitin ligase that operates under normal conditions with its activity being repressed while residing in the cytosol. Its structure includes an ubiquitin-like domain at the N-terminus and falls under the RING-between-RING group of E3 ubiquitin ligases (Figure 8). When in a physiological state, Parkin adopts an auto-inhibited conformation.

Autosomal recessive Parkinson's disease is frequently attributed to loss-of-function mutations in the Parkin gene, and a staggering number of over 120 different mutations in this gene have been associated with the development of the disease (26).

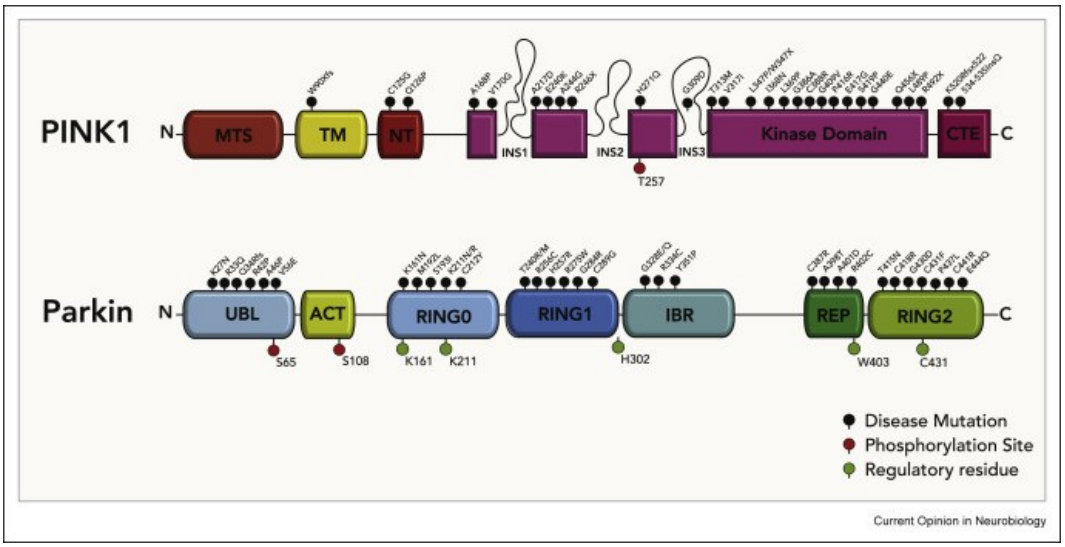

Figure 7; Domain organization of human PINK1 and Parkin. Schematic representations of the mitochondrial kinase PINK1 and the RBR-E3 ubiquitin-protein ligase Parkin. Individual domains are color coded and labelled: MTS, mitochondrial targeting sequence; TM, transmembrane domain; NT, N-terminal, regulatory domain; INS, insertion; CTE, C-terminal extension; UBL, ubiquitin-like domain; ACT, activating element; RING, really interesting new gene domain, IBR, in-between-RING domain; REP, repressor element; fs, frameshift mutation. PINK1, PTEN-induced kinase 1; RBR-E3, RING-IBR-RING-E3 Selected PINK1 and Parkin human disease mutations, the phosphosites and regulatory residues referred in the text are highlighted in the domain structure as black, red and green, respectively. Figure obtained from reference (27).

As described earlier, in normal cellular conditions, PINK1 undergoes import into mitochondria, followed by cleavage and subsequent degradation. However, when there is a loss of mitochondrial membrane potential, induced by mitochondrial uncouplers like carbonyl cyanide m-chlorophenyl hydrazine (CCCP), PINK1's import through the TIM complex is inhibited, leading to its stabilization on the outer mitochondrial membrane (OMM). In this state, full-length PINK1 becomes localized on damaged mitochondria, marking them for degradation and distinguishing them from healthy, unaffected mitochondria.

Initial experiments in immortalized cell lines established the association of Parkin with mitophagy. They demonstrated that cytosolic Parkin could be recruited to depolarized mitochondria after being exposed to CCCP.

The involvement of PINK1 and Parkin in a shared mitochondrial quality control process was suggested through various observations and experiments. Mutations in PINK1 and Parkin have been linked to autosomal recessive Parkinson's disease

(PD), and post-mortem analysis of PD patient brains has revealed an accumulation of damaged mitochondria.

Studies conducted using Drosophila with PINK1 or Parkin loss-of-function showed significant mitochondrial dysfunction, male sterility, and defects in mitochondrial morphology. However, in PINK1-knockout Drosophila, the overexpression of human PINK1 or Parkin was able to ameliorate these effects (28). Intriguingly, when Parkin was knocked out in Drosophila, the overexpression of PINK1 alone could not reverse the observed phenotype, indicating that in the mechanistic pathway, Parkin operates downstream of PINK1.

PINK1 accumulation on the OMM leads to the activation of its kinase activity. Active PINK1 phosphorylates ubiquitin and Parkin on specific serine residues, including Ser65. Phosphorylated Parkin binds to phospho-ubiquitin chains. This

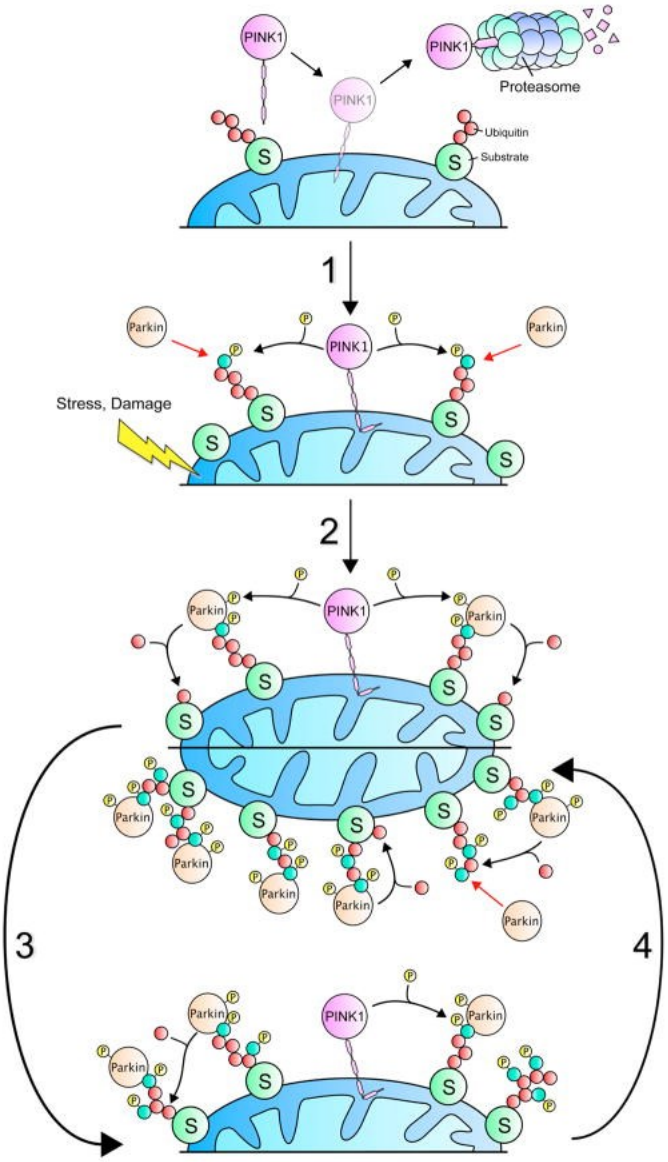

Figure 8; In basal conditions, PINK1 is imported into mitochondria, processed, and degraded by the proteasome. (1) Under mitochondrial stress, PINK1 is stabilized to the outer mitochondrial membrane where it phosphorylates ubiquitin (red circle) located on OMM proteins substrates (S). Parkin has a high affinity for phospho-ubiquitin (green circle) and translocates from the cytosol to the mitochondrial surface. (2) PINK1 activates Parkin by phosphorylation of serine 65 enhancing its E3 ubiquitin ligase activity. (3 and 4) Activated Parkin ubiquitinates OMM protein substrates and PINK1 phosphorylates ubiquitin leading to further Parkin recruitment and activation, resulting in a feedback loop which amplifies phospo-ubiquitin. Figure obtained from reference (30).

interaction enhances Parkin ubiquitin ligase activity, leading to the ubiquitination of OMM proteins and the initiation of mitophagy. (29)

Ubiquitinated proteins on the OMM serve as signals for selective autophagy, marking damaged mitochondria for degradation. Autophagosomes engulf the targeted mitochondria, and the autophagosomes subsequently fuse with lysosomes, leading to degradation through mitophagy. (30)

PINK1 and/or Parkin-Independent Mitophagy

Mitophagy is a selective process by which damaged or dysfunctional mitochondria are targeted for degradation to maintain cellular homeostasis. While the canonical pathway involving PINK1 and Parkin is well-studied, recent research suggests the existence of alternative mechanisms for initiating mitophagy independently of PINK1 and Parkin.

One of them is FUN14 domain-containing protein 1 (FUNDC1)-mediated Mitophagy. FUNDC1 is an outer mitochondrial membrane protein that can directly interact with LC3, growing factor maturating autophagosome, to facilitate mitophagy. FUNDC1-dependent mitophagy can occur without PINK1 or Parkin activation (31). As other factors, BNIP3 and BCL2L13 are identified for separately inducing mitophagy. The identification of these alternative initiation pathways for mitophagy underscores the complexity of cellular quality control mechanisms and highlights the redundancy and flexibility of cellular responses to mitochondrial stress.

Mitochondrial unfolded protein response (UPR^{mt})

The mitochondrial unfolded protein response (UPR^{mt}) is a cellular stress response pathway that is activated in response to disruptions in mitochondrial proteostasis. It aims to restore proper protein folding and function within mitochondria. This response is essential to maintain mitochondrial health and cellular viability.

The UPR^{mt} is initiated by the accumulation of unfolded or misfolded proteins within the mitochondrial matrix. Mitochondrial ribosomal proteins are particularly sensitive to stress and act as stress sensors. During mitochondrial stress, these ribosomal proteins are titrated away from their assembly role, leading to ribosome stalling and the activation of the UPR^{mt} pathway. A key regulator of the UPR^{mt} is

ATFS-1 (Activating Transcription Factor associated with Stress-1) in

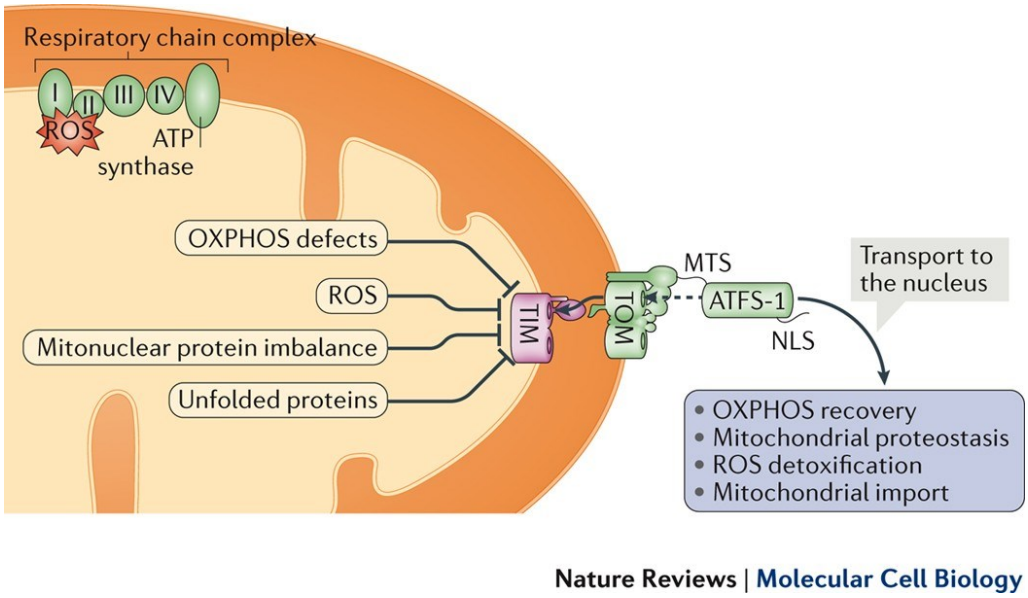

Figure 9; Oxidative phosphorylation (OXPHOS) perturbation, excessive reactive oxygen species (ROS), impaired complex assembly (mitonuclear protein imbalance) and the accumulation of misfolded proteins impair mitochondrial protein import efficiency and activate ATFS-1 (activating transcription factor associated with stress). ATFS-1 is imported into healthy mitochondria via its mitochondrial-targeting sequence (MTS), where it is degraded. If mitochondrial import efficiency is perturbed, ATFS-1 is transported to the nucleus and the mitochondrial unfolded protein response (UPR^{mt}) is activated. In the nucleus, ATFS-1 induces a number of genes that re-establish mitochondrial function and import efficiency, such as genes that promote recovery of the OXPHOS complexes, re-establish mitochondrial proteostasis by upregulating chaperones and proteases and detoxify ROS, as well as protein import components. NLS, nuclear localization sequence; TIM, translocase of the inner membrane; TOM, translocase of the outer membrane. Figure obtained from reference (33).

Caenorhabditis elegans (C. elegans) or integrated stress responses (ISR) signaling in mammals, which plays a crucial role in the response to mitochondrial proteostasis stress. These molecules transmit stress response signal from mitochondria to the nucleus to activate the expression of stress-responsive genes such as mitochondrial proteinase and chaperone (32).

Objectives of thesis

In order to specifically disentangle broad mitochondrial malfunction caused by the toxins commonly used in studies aimed at elucidating mitochondrial quality control pathways from the specific mitochondrial and cellular responses to mitochondrial damage, our lab developed a tool for the simultaneous induction and visualization of mitochondrial unfolded protein generation and accumulation in different mitochondrial sub-compartments. The aim of my thesis work has been to study the role of MDVs and mitophagy in the clearance of unfolded protein accumulated in the mitochondrial IMS or matrix, by using two cellular systems of inducible mitochondrial unfolded protein formation and accumulation generated in the lab.

Methods

Cell Culture and Transfection Procedures

U2OS, HeLa, and LentiX cell lines were cultured in Dulbecco's Modified Eagle Medium (DMEM, Invitrogen) supplemented with 4.5 mg/ml glucose, 100 µM non-essential amino acids (Invitrogen), 50 U/ml penicillin, 50 µg/ml streptomycin, and either 10% (vol/vol) fetal bovine serum (FBS, Invitrogen) or Tet-System Approved FBS (Takara). The cultures were maintained at 37 ºC in a 5% CO2 atmosphere. To ensure the absence of mycoplasma contamination, routine RT-PCR tests were conducted on all cell lines. For the induction of gene expression via the TetON system, 1 µg/ml doxycycline was introduced into the cell culture medium and renewed every 24 hours. Transfection of cells was carried out using polyethyleneimine (PEI) MAX.

DNA Construct Assembly

A previously designed Lenti MTS-mtagBFP2 plasmid was employed, where the pLJM1 vector contained mtagBFP2 downstream of a classical mitochondrial targeting sequence based on Cox8. The linearized vector without the mitochondrial targeting sequence (MTS) was generated from the lenti MTS-mtagBFP2 plasmid by digesting it with NheI-HF (NEB) and AgeI-HF (NEB) enzymes.

MTS-EGFP without a stop codon was amplified from the lenti MTS-EGFP plasmid, previously utilized in our research, along with a flexible linker sequence using Prime STAR GXL and PCR primers (CMV5 v.2 and MTS-EGFP-RV), following the manufacturer's protocol. The purified digested lenti MTS-mtagBFP2 and the amplified MTS-EGFP were subjected to seamless ligation using a homemade seamless ligation cloning extract (SLiCE) method, as described in the provided protocol (34).

In brief, a crude extract of Stbl3 competent Escherichia coli (E. coli) was mixed with SLiCE buffer containing 500 mM Tris-HCl pH 7.5, 100 mM MgCl2, 10 mM ATP, and 10 mM DTT for the ligation between the insert and vector. The seamless ligation reaction was carried out at 37 °C for 20 minutes.

The resulting ligation product was transformed into Stbl3 competent E. coli cells and plated onto LB plates containing 50 mg/ml Ampicillin (Sigma). After 48 hours of growth at room temperature, positive colonies were selected, diluted, and subjected to colony PCR verification. The colonies showing a positive band in

colony PCR were cultured in LB medium for 18 hours, followed by miniprep using the Kit (QIAGEN), following the manufacturer's protocol. The sequence of the miniprep product was confirmed through DNA sequencing using LightRun Tube Barcodes (Eurofin) and sequencing primers (CMV5 v.2 and pLJM1rev) before Maxiprep, conducted using the kit (Thermo Fisher Scientific).

The following primers were utilized:

MTS-EGFP-RV:

CTCCTTAATCAGCTCGCTCATTCTAGActgccatttgtctcgaggtcg

CMV5 v.2:

CAACGGGACTTTCCAAAATGTCG

pLJM1rev:

CTGTCCCTGTAATAAACCCG

In addition to this, several other plasmids were previously generated in our lab, including:

- TREtight promoter-driving empty vector for lentivirus production
- TREtight promoter-driving mitochondrial IMS or Matrix-targeting firefly luciferase WT or R188/261Q mutant conjugating FAST-myc-tag for lentivirus production
- GFP-Parkin expression vector for Retrovirus production

Virus Production and Cell Infection Protocol

For virus production, LentiX cells were employed as the packaging cell line and were co-transfected with the packaging vector psPAX2 (Addgene #12260), the envelope vector CMV promoter-driving VSVG, and the respective lentiviral vector encoding the target gene of interest. The viral supernatant was harvested and used for transduction in conjunction with 5 μg/ml polybrene. After 24 hours of transduction, cells were subjected to selection using 2 μg/ml puromycin or 20 μg/ml hygromycin, depending on the resistance marker used. Similarly, retrovirus production was conducted using a gag-pol expression vector instead of psPAX2.

The following backbone vectors were employed: pLJM1-puro vector (Addgene #91980) or pLJM1-hygro vector containing the hygromycin resistance gene in place of the puromycin resistance gene for stable expression, and pLVX-Tight-Puro vector (Takara) containing the Tetracycline-inducible promoter TREtight to enable

inducible expression via the TetON system. The pCX4pur vector was utilized as the backbone for retrovirus production.

To establish U2OS cells stably expressing the tetracycline-controlled trans-activator protein rtTA-Advanced, a limited dilution technique was employed using the FUW-M2rtTA vector (Addgene #20342).

Immunofluorescence

Immunostaining was performed by seeding cells onto 10 mm round coverslips. Cells were directly fixed with prewarmed 4% (wt/vol) paraformaldehyde (PFA) in PBS for 10 min at room temperature. Cells were permeabilized with 0.1% (wt/vol) Triton X-100 in PBS for 20 min, blocked with 1% (vol/vol) BSA in PBS for 20 min, and incubated with primary antibodies in PHEM buffer containing 2% goat serum (Sigma) for 1 hour at room temperature. Cells were then incubated with the appropriate secondary antibodies for 1 hour. The sample was mounted with Prolong Diamond (Invitrogen).

The following primary antibodies were used:
At 1:2000 dilution for TOM20 (Proteintech) and PDH (abcam), at 1:1500 for Myc-tag (Cell signaling and BD biosciences), and at 1:300 for TOM20 (Santa Cruz Biotechnology).

The following secondary antibodies were used:
At 1:750 dilution for anti-rabbit Alexa Fluor 488 (Invitrogen), anti–mouse 668 (Invitrogen), anti- rabbit 647 (Invitrogen), anti-mouse IgG2a Alexa Fluor 568 (Invitrogen), anti-mouse IgG1 Alexa Fluor 647 (Invitrogen), anti-rabbit Alexa Fluor 568 (Invitrogen).

Images were acquired using a 60X objective lenses by X63/1.4 numerical aperture (NA) oil immersion objective lenses on a Zeiss LSM900 inverted confocal microscopy. 5 stacks of 0.2 µm each was performed.

MitoQC-blue Imaging Procedure

For the purpose of live imaging, cells were carefully seeded onto 24 mm circular glass coverslips. These cells were nurtured in FluoroBrite DMEM (Invitrogen), enriched with GlutaMAX (Invitrogen), 10 mM HEPES (Invitrogen), 100 µM non-essential amino acids (Invitrogen), and 1mM sodium pyruvate (Invitrogen), along with 0.2% FBS during the imaging process. To enable the visualization of the

fluorescence-activating and absorption shifting tag (FAST), a chemical labeling tag, 3 μM TFcoral (The Twinkle Factory) was introduced into the culture medium. Subsequently, the prepared coverslips were carefully mounted onto the stage of an inverted confocal microscopy system, specifically the Zeiss LSM900 model. During the image acquisition, the emission lasers were appropriately chosen, with 405/488 nm lasers for MitoQC-blue and a 543 nm laser for TFcoral, respectively. These lasers were used in conjunction with an X63/1.4 NA oil immersion objective. To capture comprehensive data, a series of three stacks, each with a resolution of 0.2 μm, were meticulously performed.

Image Processing and Analysis Procedure

In the realm of image processing and analysis, an amalgamation of Fiji and a custom-written automated program through ImageJ macro was employed. Prior to embarking on the analysis, a crucial step entailed compiling images via maximum-intensity z-projection. Upon this compilation, the individual cellular areas within the images were meticulously enclosed and subsequently integrated into the ROI manager for streamlined analysis.

To generate the binary masked images, a meticulous approach was followed. This encompassed the elimination of all background signal via rolling ball subtraction, followed by the conversion of intensity value 0 to NaN. The threshold for the binary process was judiciously calculated based on the mean and standard deviation within the histogram of the remaining positive signals. Further refining the analysis, specific criteria were introduced pertaining to circularity, size, and intensity. These constraints were employed for the creation of masked images considering the following factors: 1) MDV definition as a vesicle smaller than a mitochondrion, 2) spherical structural consideration for mitophagosomes, and 3) the recognition that MDV- and mitophagosome-like structures surpass noise dimensions. Utilizing the masked images stemming from TOM20 and PDH-immunostaining, unique vesicle-like structures corresponding to MDVs were discerned. On the other hand, by deploying the masked images of tandem EGFP and mtagBFP2, the identification of mitophagosomal structures was achieved. These meticulous processes were systematically replicated across the individual cellular areas indicated within the ROI manager.

To quantify the recruitment of GFP-Parkin, a manual approach was adopted for counting positive cells.

Statistical Analysis Approach

All presented outcomes are represented as the mean along with the corresponding standard deviation (SD). To gauge the variation and significance across independent experiments, a rigorous analytical methodology was employed. Specifically, a one-way ANOVA test was conducted, supplemented by Bonferroni's post hoc test, which was subsequently followed by Tukey's honestly significant difference (HSD) test. The total count of independent experiments is duly denoted as 'n'.

Results

1.1 Induction of unfolded proteins in mitochondria results in MDV accumulation

We first decided to measure whether mitochondrial unfolded protein accumulation induces the formation of mitochondrial derived vesicles (MDVs). Our lab developed a U2OS model for mitochondrial unfolded protein accumulation by introducing into mitochondria an exogenous unfolded protein, a dual-mutated firefly luciferase R268/281Q ($fLuc^{RQ}$) showing lower structural stability and prone to aggregation (35). $fLuc^{RQ}$ was specifically and precisely targeted into mitochondrial IMS or matrix, here referred to as IMS mutant (IMS M.) or MTS mutant (MTS M.). These mitochondrial unfolded proteins IMS M. and MTS M. were fused to a chemical labeling tag Fluorescence-Activating and absorption Shifting Tag (FAST) for live-cell imaging and to a Myc-tag epitope for immunostaining. To chase the stress responses from the beginning and avoid the accumulation of cellular damage by continuous mitochondrial unfolded protein generation, IMS M. and MTS M. were placed under the control of a TetON system. We then compared these cell lines to the EV cells similarly treated with doxycycline by staining them for established markers of MDVs. Previous reports using advanced super resolution microscopy indicated that MDVs are distinct structures of 100-150nm in diameter. MDVs carry specific cargoes, including the mitochondrial protein translocator of the outer membrane (TOM) complex and pyruvate dehydrogenase (PDH), the mitochondrial matrix enzyme catalyzing the decarboxylation of pyruvate to acetyl coenzyme A. These two cargoes are mutually exclusive i.e., MDVs that are TOM20+ are negative for PDH and vice versa.

Albeit we could find a small number of TOM20+, PDH- as well as PDH+, TOM20- MDVs in EV U2OS cells upon treatment with doxycycline, the number of these vesicles were increased in cells expressing the $fLuc^{RQ}$ aggregation prone mutants. In particular, we found that TOM20+ MDVs accumulated when we induced expression of $fLuc^{RQ}$ in the IMS, whereas we could observe a small but significant induction of PDH+ MDVs when cells expressed $fLuc^{RQ}$ in the matrix (Fig. 10).

These data suggest that in the EV control cell formation of PDH+ and TOM20+ MDVs occurs to a level that was picked up by our experimental setup of immunofluorescence. Furthermore, PDH+ MDVs accumulate when unfolded

proteins are induced in the matrix, whereas TOM20+ MDV are a specific response to mitochondrial unfolded proteins accumulation in IMS rather than in matrix.

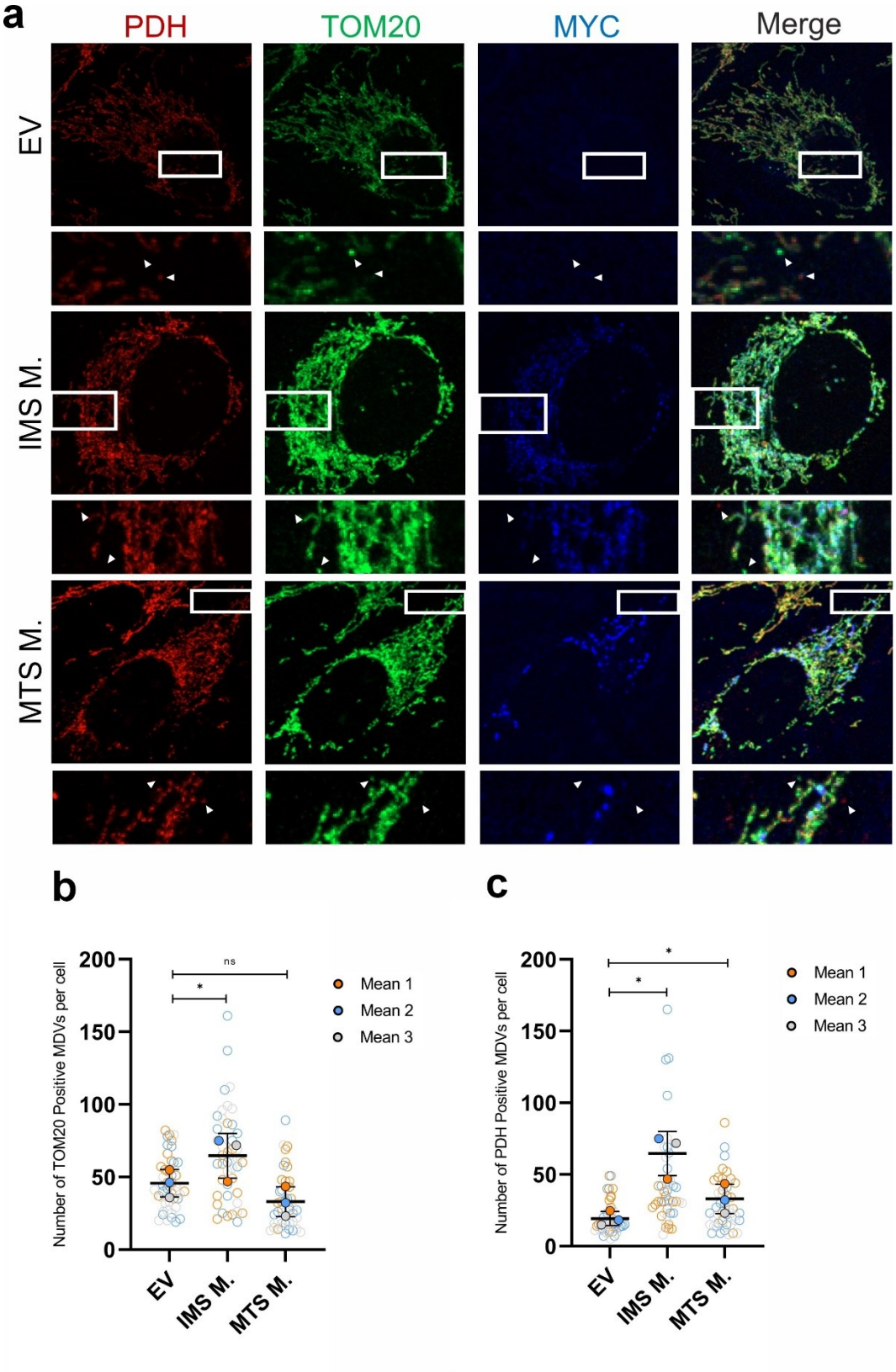

*Figure 10. TOM20+ MDVs accumulate upon induction of unfolded protein aggregates in the mitochondrial IMS. (a) Cells of the indicated genotype were immunostained using TOM20, PDH, Myc-tag antibodies. The white rectangles illustrate the magnified parts of the image. The absence or presence of the MDVs are shown with white triangles. Cells were treated with doxycycline for 48 hours to induce expression of the mitochondrial unfolded proteins. EV: empty vector, IMS M.: mitochondrial IMS targeting luciferase mutant with FAST and myc-tag, Matrix M.: mitochondrial matrix targeting luciferase mutant with FAST and myc-tag. (b, c) Quantitative analysis of TOM20+ MDVs (b), PDH+ MDVs (c). Data of individual cells from 3 independent experiments (for each experiment 15 cells were counted) are plotted as empty circles, and filled circles indicate the average of individual experiments. Error bars indicate S.D. *: P< 0.05, n.s: non-significant in an ANOVA test.*

2.1 Generation of a sensor for real time imaging of mitophagy

Autophagy is an important mechanism for the degradation of inactive, nonessential, or damaged cellular components. Selective mitochondrial autophagy, called mitophagy, is a common mechanism of mitochondrial quality control. However, it is unclear whether mitochondrial unfolded protein accumulation results in mitophagy. A limitation in the measurement of mitophagy is the lack of specific sensors that allow imaging of the process compatibly with other fluorophores in real time. Common autophagy biosensors have been designed using tandem Fluorescence Proteins with different pH sensitivity. Biosensors based on tandem fluorescent proteins retain both fluorescence when in pH is physiological. When autophagosomes cargo are targeted to the acidic lysosome, the signal of the acidic pH-sensitive fluorescent protein disappears, whereas the fluorescence of the other protein in the biosensor is retained. Thus, while these tandem fluorescence proteins fluoresce in both wavelengths at physiological pH, they display a single-color emission when they are delivered to the lysosome. To date, researchers have utilized diverse tandem fluorescent proteins, such as EGFP, YFP, CFP, RFP, mCherry, and HcRed to visualize autophagy-related pathways in live cells. In my thesis work, these tandem fluorescent pairs however were not compatible with the simultaneous imaging of the FAST tag of the fLuc^{RQ} unfolded proteins. We therefore decided to generate and characterize a mitophagy sensor based on different fluorescent protein pairs with spectral properties compatible with those of the FAST tag used here. To this end, we selected EGFP as the pH-sensitive protein that loses fluorescence in the lysosome, and mtagBFP2 as the pH-insensitive protein the fluorescence of which is sustained in acidic conditions. In order to adapt this protein pair to the measurement of mitophagy, we conjugated the tandem EGFP-mtagBFP2 to the Cox8 mitochondrial targeting sequence. We named this sensor MitoQC-blue (Figure 11a). We next verified that this sensor could detect mitophagy. To this end, we treated cells with the mitochondrial respiratory inhibitor antimycin A and the ATP synthase inhibitor oligomycin, a widely used combo treatment that induces mitochondrial depolarization and mitophagy. Upon induction of mitochondrial dysfunction, we could aptly observe the appearance of MTagBFP2-positive/ EGFP negative dot like mitochondria, indicative of mitochondria targeted to the lysosome. Indeed, the number of MitoQCblue positive dots was notably higher in cells treated

with Antimycin A/oligomycin compared with untreated ones. Thus, when mitophagy was induced, MitoQCblue could report the occurrence of mitochondria targeted to an acidic compartment where EGFP is degraded (Figure 11b).

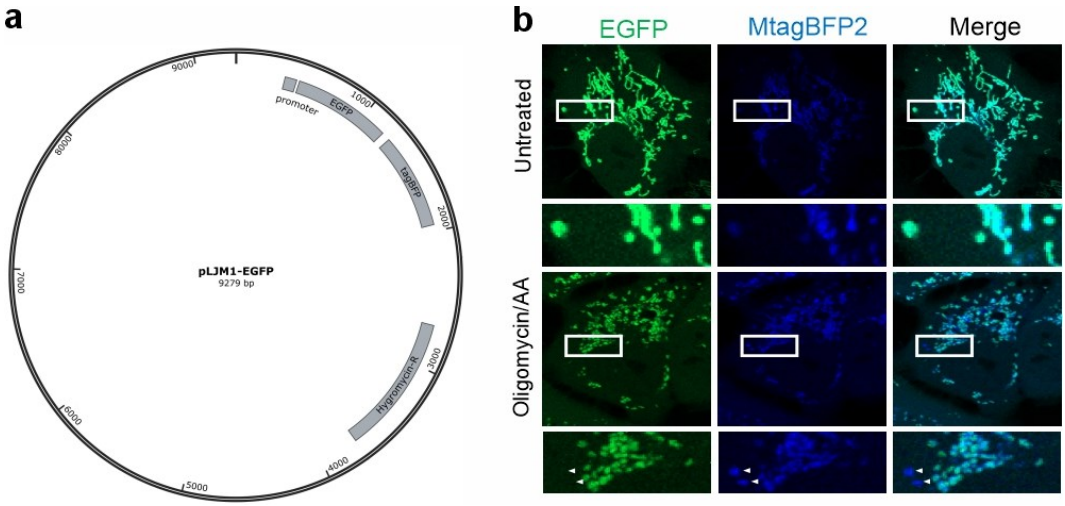

Figure 11. Real time imaging of mitophagy using new sensor. a) MitoQCblue vector map containing EGFP, MtagBFP2 and Hygromycin-resistance area. (b) Cells were treated with doxycycline for 48 hours to induce expression of mitophagy by TetON system. The white rectangles illustrate the magnified parts of the image. The absence or presence of the MTagBFP2-positive/ EGFP negative regions are shown with white triangles. The untreated cell illustrated in this figures lacks having any MTagBFP2-positive/ EGFP negative region.

2.2 Accumulation of unfolded proteins in the IMS causes mitophagy

We next used MitoQC-blue to compare mitophagy by live-imaging in EV, IMS M. and MTS M. expressing cells. We capitalized on the FAST tag of our fLUCRQ inducible construct and employed TF coral to visualize the formation of aggregates of fLUCRQ in the mitochondrial IMS and matrix. Real time imaging revealed a greater number of MTagBFP2-positive/ EGFP negative mitochondria in cells expressing IMS M. compared to EV and MTS M expressing cells (Figure 12a). Quantitative analysis confirmed that the average number of MTagBFP2-positive/ EGFP negative mitochondria were greater in IMS M. compared to the control and MTS M cells. (Figure 12b). Thus, mitochondria with unfolded proteins accumulating in the IMS are not only shedding TOM20+ MDVs, but also targeted for mitophagy.

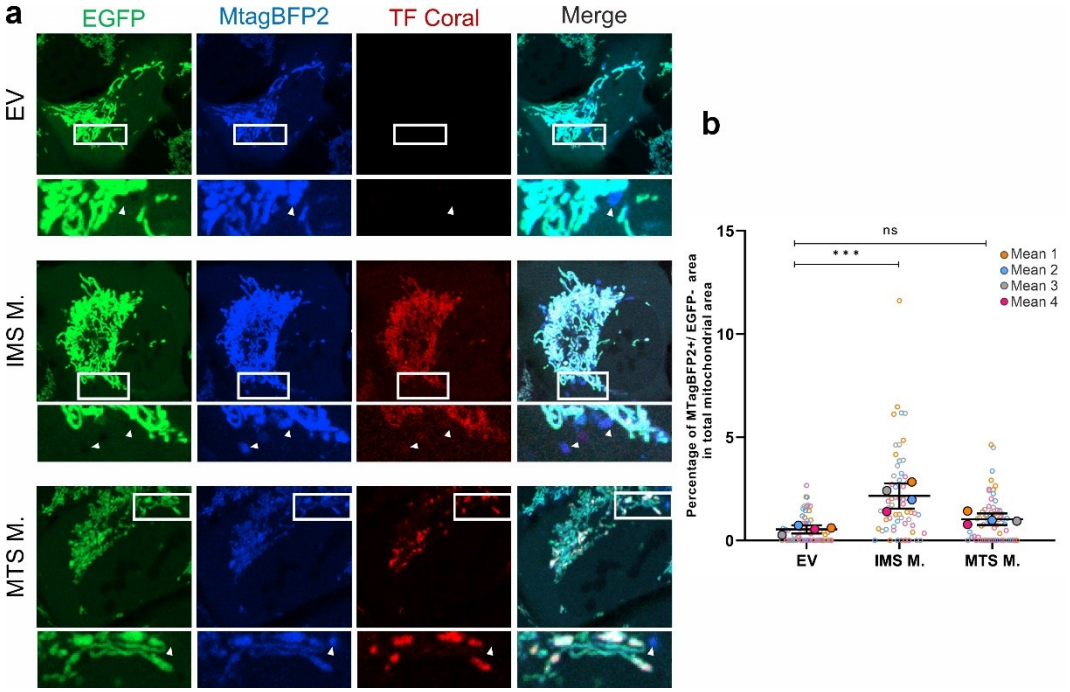

*Figure 12. Induced mitophagy via accumulation of unfolded protein. (a) Cells expressing EGFP and MtagBFP2 and absorption shifting tag (FAST), TFcoral (The Twinkle Factory) was used to track unfolded protein. The white rectangles illustrate the enlarged desired parts of the sample. The absence or presence of the MTagBFP2-positive/ EGFP negative regions are shown with white triangles. All cells were treated with doxycycline 48 hours for inducing the expression of mitochondrial unfolded protein by TetON system. IMS M.: mitochondrial IMS targeting luciferase mutant with FAST TFcoral, Matrix M.: mitochondrial matrix targeting luciferase mutant with FAST TFcoral. (b) Quantitative analysis of blue positive/green negative area. Data of individual cells from 4 independent experiments (for each experiment 15 cells were counted, total number was 60 cells), the average score is calculated among these 4 trials. Error bar indicate S.D. ***: p<0.001 in an ANOVA test.*

3.1 Accumulation of unfolded proteins in the IMS leads to Parkin recruitment on mitochondria

In the canonical mitophagy pathway, PINK1 and Parkin accumulate on depolarized or damaged mitochondria. We therefore wished to understand whether the targeting of mitochondria to lysosomes upon IMS unfolded protein accumulation was due to the activation of this pathway. We therefore examined the subcellular distribution of a GFP-parkin chimera in our cellular models of mitochondrial unfolded protein accumulation. Of note, the number of GFP-parkin dots in IMS M. expressing cells was higher than control and MTS M. expressing cells (Figure 12a). Furthermore, IMS unfolded proteins colocalized with Parkin, whereas MTS unfolded proteins did not (figure 12b). These results suggest that mitochondrial IMS unfolded

proteins lead to Parkin recruitment on mitochondria, compatible with the observed increased levels of mitophagy.

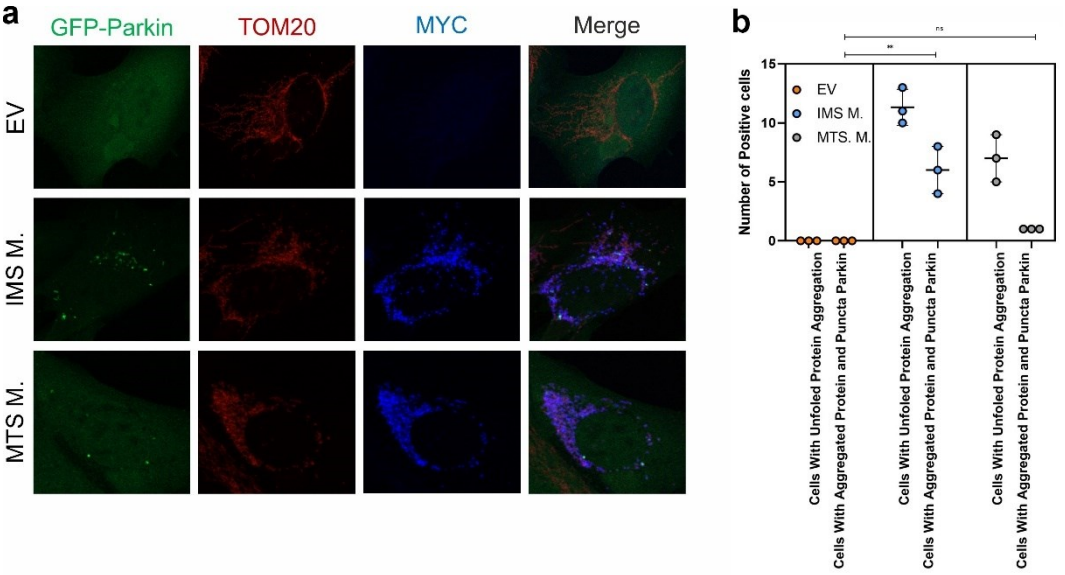

*Figure 13 Parkin Accumulation by mitochondrial unfolded protein. (a) GFP-Parkin cells were immunostained using TOM20, Myc-tag antibodies. All cells were treated with doxycycline 48 hours for inducing the expression of mitochondrial unfolded protein by TetON system. Control: empty vector, IMS M.: mitochondrial IMS targeting luciferase mutant with FAST and myc-tag, Matrix M.: mitochondrial matrix targeting luciferase mutant with FAST and myc-tag. Error bars on shown with black color. (b) Quantitative analysis of cells expressing unfolded protein and the cells having the same condition and on top of it having Parkin accumulated. Data of individual cells from 3 independent experiments (for each experiment 15 cells were counted, total number was 45 cells) were plotted as refilled cycle indicated. Error bar indicate S.D. ** for $p<0.01$, n.s: non-significant in an ANOVA test.*

Discussion

The experimental results demonstrate the interplay between imbalance of mitochondrial proteostasis and mitochondrial quality control pathways. Both quality maintenance system of mitochondria, MDVs formation and mitophagy, were activated in response to the accumulation of unfolded proteins in the mitochondrial IMS. In the case of unfolded protein accumulation in the mitochondrial matrix, only MDV formation was significantly induced.

Interestingly, MDVs formed in response to unfolded protein accumulation in the two different compartments, IMS and matrix, differ for their nature, defined on the basis of their prevalent cargo. Indeed, MDVs formed upon unfolded protein accumulation in the IMS are TOM20+ and PDH-, whereas the opposite is true for MDVs formed upon unfolded protein accumulation in the mitochondrial matrix. Whereas there is a dedicated pathway for recruitment of excess/unwanted PDH complexes into MDVs and their removal from mitochondria where unfolded proteins accumulate in the matrix remains to be understood. PDH is a key enzyme to fuel the TCA cycle with carbon units from glycolysis. The accumulation of PDH+ MDV in cells where unfolded proteins accumulate in the matrix may modulate TCA cycle in response to unbalanced proteostasis, connecting metabolism to mitochondrial quality control.

Accumulation of unfolded proteins in the IMS leads to mitochondrial membrane potential reduction (not shown). Such changes might trigger Parkin recruitment, explaining why we observe mitophagy and Parkin recruitment only in the case of cells where unfolded proteins accumulate in the IMS. How unfolded protein accumulation in the IMS leads to mitochondrial depolarization is unclear. One possibility is that the abundant shedding of TOM20 by MDVs reduces global mitochondrial protein import, causing a secondary imbalance in mitochondrial respiratory complexes and function. Similarly, why mitochondrial membrane potential is conserved when unfolded proteins accumulate in the matrix is unclear. It appears that mitochondria are indeed resilient to matrix unfolded proteins. Given that our system allows monitoring of unfolded proteins in real time, we tend to exclude the possibility that these unfolded proteins are rapidly disposed e.g., by matrix proteases. Indeed, in such a case we would observe lower levels of matrix protein aggregates, which is not the case.

While our results suggest that mitophagy in response to mitochondrial unfolded proteins in the IMS occurs via the canonical Pink-Parkin pathway, we do not have any genetic data that allows us to functionally imply it in the observed mitophagy. Indeed, we cannot exclude a role for other mitophagy mediators (BNIP3, BCL2Rambo…) in the process, or for direct mitochondria-lysosome contacts mediated for example by the Fis1-TBCD1C interaction.

References

1. Ke P.Y., 2020. Mitophagy in the Pathogenesis of Liver Diseases. Cells, 9(4): 831. Available at; https://www.ncbi.nlm.nih.gov/pmc/articles/PMC7226805/
2. Sugiura, A., McLelland, G. L., Fon, E. A., & McBride, H. M. (2014). A new pathway for mitochondrial quality control: mitochondrial-derived vesicles. The EMBO Journal, 33(19), 2142-2156. Available at; https://www.embopress.org/doi/full/10.15252/embj.201488104
3. Zoratti M. et al., 2009. Novel channels of the inner mitochondrial membrane. Biochimica et Biophysica Acta (BBA) - Bioenergetics, 1787(5),351–363. Available at: https://www.sciencedirect.com/science/article/pii/S0005272808007329?via%3Dihub
4. Walther D.M., Rapaport D., 2009. Biogenesis of mitochondrial outer membrane proteins. Biochimica et Biophysica Acta (BAA) - Molecular Cell Research, 1793(1), 42–51. Available at: https://www.sciencedirect.com/science/article/pii/S0167488908001493
5. Protasoni M., Zeviani M., 2021. Mitochondrial Structure and Bioenergetics in Normal and Disease Conditions, Int. J. Mol. Sci. 22(2), 586, 22020586. Available at: https://www.mdpi.com/1422-0067/22/2/586
6. Rizzuto R. et al., 1992. Rapid changes of mitochondrial Ca2+ revealed by specifically targeted recombinant aequorin. Nature, 358(6384), 325–327. Available at: http://www.ncbi.nlm.nih.gov/pubmed/1322496
7. Matuz-Mares D. et al., 2022. Mitochondrial Calcium: Effects of Its Imbalance in Disease. Antioxidants, 11(5), 801, 11050801. Available at: https://www.mdpi.com/2076-3921/11/5/801
8. 2010 Nature Education, Available at: https://www.nature.com/scitable/ebooks/essentials-of-cell-biology-14749010/122996679

9. Liu Y. J. et al., 2020 Mitochondrial fission and fusion: A dynamic role in aging and potential target for age-related disease, 183. Available at: https://www.sciencedirect.com/science/article/pii/S0047637420300063
10. Züchner S. et al., 2004. Mutations in the mitochondrial GTPase mitofusin 2 cause Charcot-Marie-Tooth neuropathy type 2A. Nature Genetics, 36(5),449–451. Available at: http://www.nature.com/doifinder/10.1038/ng1341
11. Koshiba T. et al., 2004. Structural Basis of Mitochondrial Tethering by Mitofusin Complexes. Science, 305(5685), 858–862. Available at: http://www.ncbi.nlm.nih.gov/pubmed/15297672
12. Song Z. et al., 2009. Mitofusins and OPA1 mediate sequential steps in mitochondrial membrane fusion. Molecular biology of the cell, 20(15), 3525–32. Available at: http://www.ncbi.nlm.nih.gov/pubmed/19477917
13. Chan D.C., 2012. Fusion and Fission: Interlinked Processes Critical for Mitochondrial Health. Annual Review of Genetics, 46(1), 265–287. Available at: Fusion and Fission: Interlinked Processes Critical for Mitochondrial Health | Annual Review of Genetics (annualreviews.org)
14. Ishihara N. et al., 2009. Mitochondrial fission factor Drp1 is essential for embryonic development and synapse formation in mice. Nature Cell Biology, 11(8), 958–966. Available at: http://www.ncbi.nlm.nih.gov/pubmed/19578372
15. Otera H. et al., 2010. Mff is an essential factor for mitochondrial recruitment of Drp1 during mitochondrial fission in mammalian cells. The Journal of Cell Biology, 191(6), 1141–1158. Available at: http://www.ncbi.nlm.nih.gov/pubmed/21149567
16. Soubannier V., McLelland, G.L., et al., 2012. A vesicular transport pathway shuttles cargo from mitochondria to lysosomes. Current Biology, 22(2), 135–141. Available at: http://dx.doi.org/10.1016/j.cub.2011.11.057
17. Langer T., M. McBride, H. et al., 2021. MIROs and DRP1 drive mitochondrial-derived vesicle biogenesis and promote quality control. Nature Cell Biology, 23,1271–1286. Available at:

https://www.nature.com/articles/s41556-021-00798-4

18. Kameoka S., et al., 2018. Phosphatidic acid and cardiolipin coordinate mitochondrial dynamics. Trends Cell Biol. 28(1), 67–76. Available at: https://pubmed.ncbi.nlm.nih.gov/28911913
19. Kleele T. et al, 2021. Distinct fssion signatures predict mitochondrial degradation or biogenesis. Nature 593, 435–439. Available at: https://pubmed.ncbi.nlm.nih.gov/33953403
20. Nagashima S. et al, 2020. Golgi-derived PI(4)P-containing vesicles drive late steps of mitochondrial division. Science 367, 1366–1371. Available at: https://pubmed.ncbi.nlm.nih.gov/32193326
21. McLelland G. L., Soubannier V., Chen, C. X., McBride H. M., Fon E. 2014. A. Parkin and PINK1 function in a vesicular trafficking pathway regulating mitochondrial quality control. EMBO J. 33, 282–295. Available at: https://pubmed.ncbi.nlm.nih.gov/24446486
22. Matheoud D. et al, 2016. Parkinson's disease-related proteins PINK1 and Parkin repress mitochondrial antigen presentation. Cell 166, 314–327. Available at: https://doi.org/10.1016/j.cell.2016.05.039
23. Bruderek M. et al, 2018. IMiQ: a novel protein quality control compartment protecting mitochondrial functional integrity. Mol. Biol. Cell 29, 256–269. Available at: https://www.molbiolcell.org/doi/10.1091/mbc.E17-01-0027
24. Thomas R.E. et al., 2014. PINK1-Parkin Pathway Activity Is Regulated by Degradation of PINK1 in the Mitochondrial Matrix A. van der Bliek, ed. PLoS Genetics, 10(5), p.e1004279. Available at: http://dx.plos.org/10.1371/journal.pgen.1004279
25. Fedorowicz M.A. et al., 2014. Cytosolic cleaved PINK1 represses Parkin translocation to mitochondria and mitophagy. EMBO reports, 15(1), 86–93. Available at: https://www.embopress.org/doi/full/10.1002/embr.201337294
26. Durcan T.M., Fon, E.A., 2015. The three "P"s of mitophagy: PARKIN, PINK1, and post-translational modifications. Genes & Development, 29(10), 989–999. Available at:

https://doi.org/10.1016/j.ceb.2017.03.013

27. Agarwal S., Muqit M. M. K., 2022. PTEN-induced kinase 1 (PINK1) and Parkin: Unlocking a mitochondrial quality control pathway linked to Parkinson's disease. Current Opinion in Neurobiology, 111-119. Available at: https://doi.org/10.1016/j.conb.2021.09.005
28. Yang Y. et al., 2006. Mitochondrial pathology and muscle and dopaminergic neuron degeneration caused by inactivation of Drosophila Pink1 is rescued by Parkin. Proceedings of the National Academy of Sciences of the United States of America, 103(28), 10793–10798. Available at: https://doi.org/10.1073/pnas.0602493103
29. Kazlauskaite A, Kondapalli C, Gourlay R, et al., 2014. Parkin is activated by PINK1-dependent phosphorylation of ubiquitin at Ser65. Biochem J., 460(1):127-139. Available at: https://portlandpress.com/biochemj/article/460/1/127/46544/Parkin-is-activated-by-PINK1-dependent
30. Pickles S, Vigie P, Youle RJ, 2018. Mitophagy and Quality Control Mechanisms in Mitochondrial Maintenance. Curr Biol, 28(4):R170-R185. Available at: https://doi.org/10.1016/j.cub.2018.01.004
31. Chen M., Chen Z., Wang Y., et al, 2016. Mitophagy receptor FUNDC1 regulates mitochondrial dynamics and mitophagy. Autophagy. 12(4): 689-702. Available at: https://doi.org/10.1080/15548627.2016.1151580
32. Haynes C. M., Fiorese C. J., Lin Y. F., 2013. Evaluating and responding to mitochondrial dysfunction: the mitochondrial unfolded-protein response and beyond. Trends Cell Biol.;23(7): 311-318. Available at: https://doi.org/10.1016/j.tcb.2013.02.002
33. Haynes C. M., Shpilka T., 2018. The mitochondrial UPR: mechanisms, physiological functions and implications in ageing. Nature Reviews Molecular Cell Biology; volume 19, 109–120. Available at: https://www.nature.com/articles/nrm.2017.110

34. Zhang Y., Werling U., and Edelmann W., 2015. Seamless Ligation Cloning Extract (SLiCE) Cloning Method. Methods Mol Biol. 1116: 235–244. Available at: https://www.ncbi.nlm.nih.gov/pmc/articles/PMC4672941
35. Gupta R., Kasturi P., Bracher A., et al, 2011. Firefly luciferase mutants as sensors of proteome stress. Nature Methods; 8, 879–884. Available at: https://www.nature.com/articles/nmeth.1697